WWW.IJRPR.COM

International Journal of Research Publication and Reviews

Journal homepage: www.ijrpr.com ISSN 2582-7421

DESIGN AND ANALYSIS OF 6G MICROSTRIP PATCH ANTENNA FOR INTERNET OF THINGS APPLICATION

Md Sarfaraz Ahmad[1], Manish Sahu[2]

Department of Electronics and Communication Engineering, School of Research and Technology, People's University, Bhopal (M.P.),India

ABSTRACT :

Wireless technology is greatly influenced by the advanced technological development of the antenna. With the rapid expansion of Internet of Things (IoT) application in the modern communication system, the demand for micro antennas is increasing. Microstrip patch antennas are generally used in IoT applications due to its compatibility. The key benefit of the microstrip antenna is that it allows easy integration into IoT devices. Thus, in this work, rectangular microstrip patch antenna is designed and the performance will be analysed. The reality is that 6G will operate across the multiple frequency range. The 6G spectrum can be categorised into main three band low frequency band (1 GHz- 7 GHz), mid frequency band (7 GHz-20 GHz) and high frequency band (above 100 GHz). In this work, design three antenna first one on low frequency band as 5.8 GHz, and rest two antenna design on mid frequency bad on 7.125 GHz. Taking FR-4 material for substrate which has dielectric coefficient 4.4. The commercially available EM simulation software FHSS 2021R1 have been used for simulation work. Here we can see that the antenna design at 5.8 GHz gives two resonance frequency 5.78 GHz and 8.78 GHz having -15.59 dB and -4076 dB return loss respectively. Whereas antenna design on mid frequency band at 7.125 GHz also gives two resonance frequency 7.289 GHz and 10.92 GHz having return loss -47.0 dB and -31.159 dB respectively. Similarly, inverted U-notch antenna design on same mid frequency band and gives two resonance 7.38 GHz and 12.94 GHz having -15.61 dB and -13.34 dB respectively. The voltage standing ratio are all three antennas are less than 2. The impedance bandwidth of antenna first are 200 MHz and 560 MHz, second antenna gives the impedance bandwidth 310 MHz and 1.58 GHz, third antenna that is inverted U-notch gives 260 MHz and 480 MHz impedance bandwidth respectively. The gain of first, second and third antenna are 4.94 dB, 5.12 dB and 4.5 dB and directivity 6.54 dB, 6.687 dB, 6.675 dB respectively. The all three-antenna radiation efficiency 69.22 %, 69.85 % and 60.12 % respectively. The result of all three antenna compare with the requirement of 6G antenna and IoT services. Therefor these antennas appropriate for 6G and IoT services.

Keywords: Wireless Communication, Permittivity, Directivity, 6G Microstrip Antenna, IoT services.

1. Introduction :

An antenna is a tool used in free space for electromagnetic wave transmission and reception. Antennas are divided into two categories: passive and active. Devices that are reciprocal are passive antennas. The reciprocal devices are not the active antenna. The nine kinds can be used to classify antennas. Active antennas, antenna arrays, dielectric antennas, microstrip antennas, lens antennas, wire antennas, aperture antenna reflector antennas, and leaky wave antennas are among the varieties of these antennas. The antenna types differ in terms of their structures and feeding techniques. Deschamps originally put up the idea of microstrip radiators in 1953. It is possible to create microstrip antennas by printed circuit method. You can use a method called photolithographic technology to print precise dimensions on PCBs. The cost of manufacturing a microstrip antenna is cheap. Because the design mask in photolithography can be reused as much as possible, fabrication can be carried out in the same way as with a photocopy machine. Microstrip antenna has narrow bandwidth. Usually for rectangular microstrip antenna, the bandwidth is below 5%. It is also having low gain.

1.1 Internet of Things

The term "Internet of Things" (IoT) refers to a computer network that has incorporated technologies to facilitate information communication between devices in a wireless environment. By facilitating wireless connection throughout the network, IoT makes it possible for these devices to be remotely controlled, which has some positive effects on the economy and efficiency. IoT is reported in various publications to have a reasonable data throughput, be inexpensive, and operate in the frequency range of 100 MHz to 5.8 GHz. Everything with internet connectivity is categorized under the name "Internet of Things," which covers more ground than just desktop and mobile devices. In today's world of wireless telecommunications, the Internet of Things (IoT) standard is evolving quickly. When properly built, the antenna can significantly enhance the overall performance and requirements of a wireless communication system, making it one of the most crucial parts of the system. Because of their precision applications in the microwave frequency range, low profile, lightweight, and adaptability, microstrip patch antennas are commonly utilized in Internet of Things applications. Antenna downsizing has the benefit of being simple to integrate into frequently tiny and compact Internet of things devices.

1.2 Feeding Techniques

There are four feeding techniques that can be used when design the microstrip antenna. There is coaxial probe / probe coupling, microstrip insert feed, proximity (Electromagnetically) coupled microstrip antenna, aperture couple microstrip antenna feed given by [8]. In this work an insert feeding method is used the design of our proposed antenna.

1.3 Microstrip line

Microstrip line is a conductor having of width W which printed on a thin grounded dielectric substrate of thickness h and relative permittivity ε_r . Microstrip line geometry is shown below.

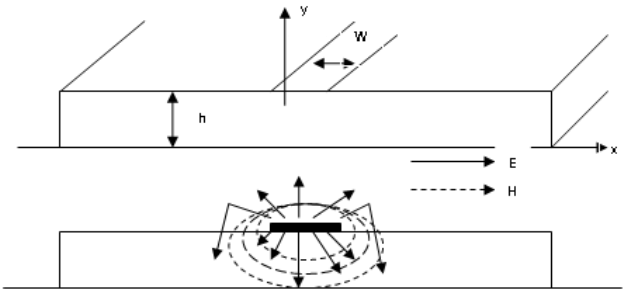

Figure 1.1 Microstrip line

The effective dielectric constant can be calculated by using following equation;

$$\varepsilon_{eff} = \frac{(\varepsilon_r + 1)}{2} + \frac{(\varepsilon_r - 1)}{2}\left[1 + 12\frac{h}{W}\right]^{-\frac{1}{2}} \quad \text{Eqn. 1.1}$$

Put the value of width and thickness of microstrip antenna in following equation and find out characteristic impedance Z_0.

$$Z_0 = \begin{cases} \frac{60}{\sqrt{\varepsilon_{eff}}}\ln\left[\frac{8h}{W} + \frac{W}{4h}\right] & for\ W/h \le 1 \\ \frac{120\pi}{\sqrt{\varepsilon_{eff}}\left\{\frac{W}{h} + 1.393 + 0.667\ln\left(\frac{W}{h} + 1.444\right)\right\}} & for\ W/h \ge 1 \end{cases} \quad \text{Eqn. 1.2}$$

Instead of using the analysis formula as above, the synthesis formula is available for finding w/h and ε_{eff} f and ε_r are known. The final formula is given by;

$$\frac{W}{h} = \begin{cases} \frac{8e^A}{e^{2A} - 2} & W/h < 2 \\ \frac{2}{\pi}\left[B - l - \ln(2B-1) + \frac{\varepsilon_r - 1}{2\varepsilon_r}\left\{\ln(B-1) + 0.39 - \frac{0.61}{\varepsilon_r}\right\}\right] & W/h > 2 \end{cases} \quad \text{Eqn. 1.3}$$

$$A = \frac{Z_0}{60}\sqrt{\frac{\varepsilon_r + 1}{2\varepsilon_r}} + \frac{\varepsilon_r - 1}{\varepsilon_r + 1}\left[0.23 + \frac{0.11}{\varepsilon_r}\right] \quad \text{Eqn. 1.4}$$

$$B = \frac{377\pi}{2Z_0\sqrt{\varepsilon_r}} \quad \text{Eqn. 1.5}$$

$$L = \frac{\phi(\pi/180)}{\sqrt{\varepsilon_{eff}}k_0} \quad \text{Eqn. 1.6}$$

$$k_0 = \frac{2\pi f}{c} \quad \text{Eqn. 1.7}$$

The matching impedance can be calculated by using following equation.

$$Z_0 = \sqrt{(Z_1 Z_2)} \quad \text{Eqn. 1.8}$$

The following table represent of comparisons between some feed methods are used for design microstrip patch antenna.

Table 1.1 Comparison of different feeding methods

Characteristics	Line Feed	Coaxial Feed	Aperture Coupled	Proximity Coupled
Configuration	Coplanar	Non-planar	Planar	Planar
Spurious Feed Radiation	More	More	More	More
Polarization Purity	Good	Good	Excellent	Poor
Ease of Fabrication	Easy	Soldering and drilling needed	Poor	Poor
Reliability	Better	Poor due to soldering	Good	Good
Impedance Matching	Easy	Easy	Easy	Easy
Bandwidth	2-5%	2-5%	20%	13%

2. Literature Review

Anchidin et al. (2023) emphasize the crucial role of efficient antennas in IoT, proposing a new design for improved long-range and low-error communication at 868 MHz, achieving a reflection coefficient of 34.3 dB and 20 MHz bandwidth.
Vyas and Salim (2022) explore novel antenna designs for 5G and potential 6G systems, focusing on a tooth-shaped patch antenna for radar applications at 300 GHz, achieving a gain of 9.45 dB and significant bandwidth.
Elijah and Mokayef (2020) discuss the use of microstrip patch antennas in IoT, comparing conventional and U-shaped designs, with the latter showing improvements in bandwidth and gain suitable for frequencies from 100 MHz to 5.8 GHz.
Chen et al. (2019) investigate the mutual coupling effects in 5G mmWave handsets, noting that reducing coupling can enhance antenna performance by improving isolation and realized gain.
Qamar et al. (2019) analyze mmWave path loss models for urban environments, concluding that the close-in (CI) model performs better in predicting network performance under line-of-sight conditions.
Hui et al. (2018) review new error-correcting codes in 5G, such as LDPC and polar codes, which offer advantages over 4G in terms of reliability and efficiency.
Tataria et al. (2021) provide a holistic overview of 6G systems, focusing on the need for wider spectrum utilization, advanced antenna designs, and new core network architectures to meet future communication demands.
Aqlan et al. (2020) present a high-gain circularly polarized resonant cavity antenna for 300 GHz, achieving a 16.2 dBic gain, suited for 6G sub-terahertz applications.
Saad et al. (2020) outline a vision for 6G that goes beyond high-frequency spectrum exploration, highlighting the integration of emerging technologies to support a diverse range of applications.
Letaief et al. (2019) discuss the role of AI in 6G, emphasizing its importance in network optimization and the provision of ubiquitous AI services.
Jia et al. (2023) introduce an antenna-integrated glass interposer for 6G, demonstrating excellent electrical performance and integration potential for D-band applications.
J. V et al. (2023) examine reconfigurable intelligent surfaces (RIS) for 6G, proposing algorithms to improve phase alignment and reduce bit error rates.
Mahpatra et al. (2023) present designs for circular patch antennas achieving broad bandwidths, suitable for 6G applications.
Omi et al. (2023) describe a CPW-fed ultra-wideband antenna for 23–150 GHz with high efficiency and gain, applicable for advanced 5G and 6G communications.
Bhutiani and Tadas (2023) discuss the development of 6G antennas capable of operating at high frequencies up to 1 THz, highlighting the need for new designs to support high-speed data transfer.
Saeed and Nwajana (2023) propose a terahertz antenna with a high bandwidth of 44 GHz, designed for future high-frequency communication needs.
Prasetyo et al. (2023) explore the use of optimization strategies to enhance the bandwidth of planar monopole antennas, achieving broad operational ranges suitable for beyond 5G and 6G applications.
Tiwari et al. (2023) design a modified antenna for 5G-6G infrastructure, achieving efficient transmission in the W and D bands with high return loss and gain, indicating its potential for future high-frequency networks.
Kumar et al. (2023) discuss the design of a fractal-inspired MIMO antenna for sub-6 GHz applications, demonstrating high gain and efficiency for IoT and wireless communication.

3. Research Methodology

3.1 Tools and Materials Used

First read some literature related to my proposed work Design and Analysis of 6G Microstrip Patch Antenna for Internet of Things Application. Then find the problem regarding the related published work last 2-3 years and set our target for doing work as per requirement of present and future scenario point of view. Fragment of my proposed work shown as flow diagram which is shown in Figure.3.1.

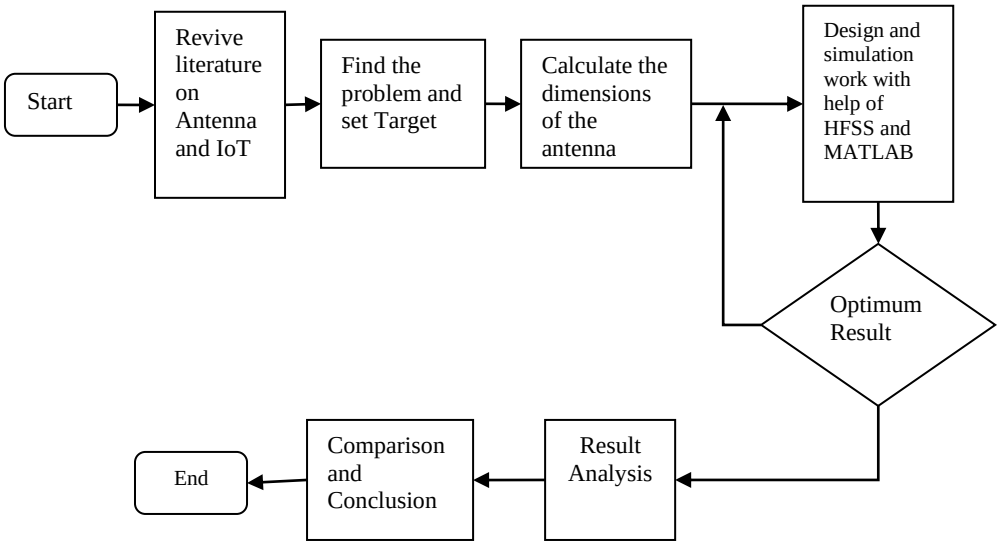

Figure 3.1 Fragment of our proposed work

3.2 Methods of Analysis

This section provides a quick explanation and derivation of many widely used models for building microstrip patch antennas. Transmission line, multiple network, method of moment, finite element, spectral domain, cavity, and finite difference time domain models are a few examples of models. Here transmission line model use for dimension calculation point of view.

3.2.1 Transmission Line Model

Transmission line model is very simple and easy to understanding. In this method two slots represent a patch and work as line resonator that occur fringing field by variation of radiating field.

The width and length of the antenna in this model are separated as transmission lines, and the thickness of the antenna is h. This is because the microstrip patch antenna is made up of two slits, the first of which is known as the radiating patch and the second of which represents the ground patch. The homogeneous line of two dielectrics, usually the substrate and air, is absent from the microstrip. Figure demonstrates that some electric field lines are in the air and that the majority of the lines are in the substrate. Because the phase velocities in the air and the substrate would differ, the transmission line's output cannot support pure TEM mode of transmission.

The width of microstrip patch can be calculated by using following equation. Where W is width of microstrip patch, C is the velocity of light, ε_r is the dielectric constant of the antenna substrate and f_0 is design frequency of the microstrip patch antenna.

$$W = \frac{C}{2 f_0 \sqrt{\frac{(\varepsilon_r + 1)}{2}}} \quad \text{Eqn. 3.1}$$

$$\varepsilon_{eff} = \frac{(\varepsilon_r + 1)}{2} + \frac{(\varepsilon_r + 1)}{2}\left[1 + 12\frac{h}{W}\right]^{-\frac{1}{2}} \quad \text{Eqn. 3.2}$$

$$\frac{\Delta L}{h} = 0.412 \frac{\left(\varepsilon_{eff} + 0.300\right)\left(\frac{W}{h} + 0.262\right)}{\left(\varepsilon_{eff} - 0.258\right)\left(\frac{W}{h} + 0.813\right)} \quad \text{Eqn. 3.3}$$

$$L = \frac{c}{2 f \sqrt{\varepsilon_{eff}}} - 2\Delta L \quad \text{Eqn. 3.4}$$

$$L_g = L + 6h \quad \text{Eqn. 3.5}$$

$$W_g = W + 6h \quad \text{Eqn. 3.6}$$

Where W_g and L_g represent the finite ground plane width and length.
The following figure shows the current flow direction in the microstrip antenna and equivalent circuit of the microstrip antenna.

Figure 3.2 Microstrip patch and its equivalent circuit

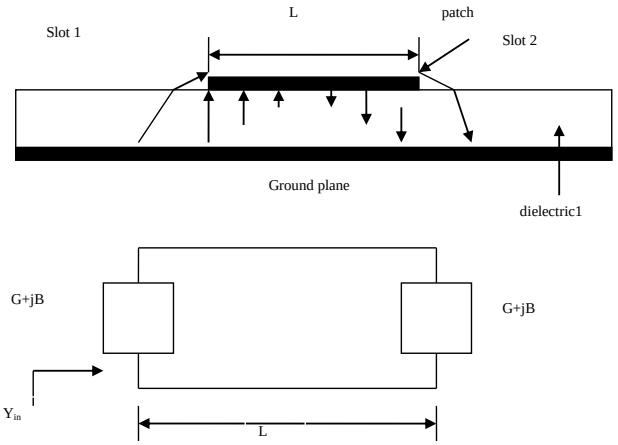

Input admittance can be calculated by following equation;

$$Y_{in} = Y_{slot} + Y_0 \frac{Y_{slot} + jY_0 \tan\beta(L+\Delta l)}{Y_0 + jY_{slot} \tan\beta(L+\Delta l)} \quad \text{Eqn. 3.7}$$

At resonance, $in\ Y = 2G$ Eqn. 3.8

As per Harrington, the conductance, for parallel radiator is given by

$$G_1 = \frac{W}{120\lambda_0}\left[1 - \frac{(kh)^2}{24}\right], \frac{h}{\lambda_0} < \frac{1}{10} \quad \text{Eqn. 3.9}$$

$$k = \frac{2\pi f}{c} \quad \text{Eqn. 3.10}$$

The calculation of the inset fed is shown in the equations (3.11) which show the resonant input resistance for the microstrip patches.

$$R_{in}(L=l) = \frac{1}{2(G_1 \pm G_{12})}\cos^2\left(\frac{\pi l}{L}\right) \quad \text{Eqn. 3.11}$$

L is the length of the patch, l is the length of the inset, G1 is the conductance of the microstrip radiator and G_{12} is the mutual conductance between the two slots. The conductance of the radiator is calculated using equation (3.12) is the current excited into the microstrip patch.

$$G_1 = \frac{I_1}{120\pi^2} \quad \text{Eqn. 3.12}$$

$$I_1 = \int_0^{\pi}\left[\frac{\sin\left(\frac{k_0 W}{2}\cos\theta\right)}{\cos\theta}\right]^2 \sin^3\theta \quad d\theta \quad \text{Eqn. 3.13}$$

The mutual conductance of the two slots (both sides of the feed) can be calculated using equation (3.14).

$$G_{12} = \frac{1}{120\pi^2}\int_0^{\pi}\left[\frac{\sin\left(\frac{k_0 W}{2}\cos\theta\right)}{\cos\theta}\right]^2 J_0(k_0 L\sin\theta)\sin^3\theta \quad d\theta \quad \text{Eqn. 3.14}$$

For insert length calculation simply put the value of dielectric constant and length of the patch of the microstrip patch antenna in following equation.

$$\ell = 10^{-4}\left(\begin{matrix}0.001699\,\varepsilon_r^{\,7} + 0.13761\,\varepsilon_r^{\,6} - 6.1783\,\varepsilon_r^{\,5} + 93.187\,\varepsilon_r^{\,4} \\ -682.69\,\varepsilon_r^{\,3} + 2561.9\,\varepsilon_r^{\,2} - 4043\,\varepsilon_r + 6697\end{matrix}\right)\frac{L}{2} \quad \text{Eqn. 3.15}$$

where:

ε_r = Permittivity of the dielectric
L = Length of the microstrip patch

3.2.2 Finite Element Method (FEM)

Here this method used for calculation of radiation field. Configurations that are volumetric can be used with the FEM. Using this method, all regions of interest are separated into a number of volume elements or finite surfaces based on the planar or volumetric features that need to be examined. These defining units, also referred to as finite elements, can be any well-defined geometric shape; curved geometry is even appropriate. The complete conducting patch, which is separated into several subsections, is modeled using basic functions. By breaking down the problem into two boundary value problems—one involving Laplace's equation and an inhomogeneous boundary, and the other related to an inhomogeneous wave equation and an inhomogeneous boundary condition-it is possible to solve wave equations with inhomogeneous boundary conditions.
A strong computer method for solving differential and integral equations is finite element modeling (FEM). The domain in question can be understood as a collection of elementary geometric objects, known as finite elements, which provide the approximation functions. The FEM method discretizes the problem using finite elements: tetrahedral, hexahedral, or prism elements for three-dimensional problems, and quadrangle or triangle elements for two-dimensional problems. Piecewise approximation is used by FEM models to solve several differential equations, yielding accurate answers in a timely manner. First-order nodal basis functions and their edge elements basis can be used to increase accuracy. The time harmonic vector wave equations are utilized for the three-dimensional modeling of a microstrip patch antenna. Since antennas work with electromagnetic waves, it is necessary to consider Maxwell's equations in order to obtain the vector wave equations, which are shown below.

$$\nabla \times B = -j\omega B \quad \text{Eqn. 3.16}$$

and

$$\nabla \times H = J_s + \sigma E + j\omega D \quad \text{Eqn. 3.17}$$

where

$$\mathrm{D} = \varepsilon_r' \varepsilon_0 E \quad \text{Eqn. 3.18}$$

and

$$\mathrm{B} = \mu_r \mu_0 H \quad \text{Eqn. 3.19}$$

In the above equations, H is the magnetic field intensity, E is the electric field intensity and ω is the operating frequency. Also, ε_0 and μ_0 is the permittivity and permeability of free space, whereas, ε_r and μ_r are the relative permittivity and relative permeability respectively. The vector wave equation for E and H is given by

$$\nabla \times \left(\frac{1}{\mu_r} \nabla \times E\right) - k_0^2 \varepsilon_r E = -j k_o \eta_0 J_S \quad \text{Eqn. 3.20}$$

And

$$\nabla \times \left(\frac{1}{\varepsilon_r} \nabla \times H\right) - k_0^2 \mu_r H = \nabla \times \left(\frac{1}{\varepsilon_r} J_S\right) \quad \text{Eqn. 3.21}$$

where J_S is the current source,

$$\varepsilon_r = \varepsilon_r' - j\frac{\sigma}{\omega \varepsilon_0} \quad \text{Eqn. 3.22}$$

And

$$k_0 = \omega\sqrt{\varepsilon_0 \mu_0} \quad \text{Eqn. 3.23}$$

Where k_o is the wave number of the free space.
Let us examine the substrate's dimensions so that, relative to the dielectric wavelength λ, the substrate's height, h, is extremely small. Because of the extremely low substrate height, the field fluctuation along the height is therefore regarded as constant. This means that only the transverse magnetic (TM) mode is taken into consideration because the electric field is normal to the patch's surface. As a result, the electric field will be parallel to the ground plane's surface. The patch's four side walls will be perfectly conducting magnetic walls, while its top and bottom walls are layers of perfectly electric conducting material. Let ε_r is the dielectric constant of the substrate and is smaller than the edges of the patch. The homogenous wave equation for the vector potential A_x is given by

$$\nabla^2 A_x + \mathrm{k}^2 A_x = 0 \quad \text{Eqn. 3.24}$$

The solution for this equation using the separation of variables is given as

$$A_X = [A_1 cos(k_x x) + B_1 sin(k_x x)].\left[A_2 cos\left(k_y y\right) + B_2 sin\left(k_y y\right)\right].[A_3 cos(k_z z) + B_3 sin(k_z z)] \quad \text{Eqn. 3.25}$$

where k_x, k_y and k_z are the wave numbers along the x, y and z direction respectively. These can be determined using boundary conditions. The electric and magnetic field related to the vector potential A_x is given by

$$E_x = -j\frac{1}{\omega\mu\varepsilon}\left(\frac{\partial^2}{\partial x^2} + k^2\right) A_x \quad \text{Eqn. 3.26}$$

$$E_y = -j\frac{1}{\omega\mu\varepsilon}.\frac{\partial^2 A_x}{\partial x \partial y}, \quad \text{Eqn. 3.27}$$

$$E_z = -j\frac{1}{\omega\mu\varepsilon}.\frac{\partial^2 A_x}{\partial x \partial z}, \quad \text{Eqn. 3.28}$$

$$H_x = 0, H_y = \frac{1}{\mu}.\frac{\partial A_x}{\partial z}, H_z = -\frac{1}{\mu}.\frac{\partial A_x}{\partial y} \quad \text{Eqn. 3.29}$$

3.3 Design Analysis

In this section, three antennas have to design at the frequency range of 6G. First antenna at 5.8 GHz and next two antennas at 7.125 GHz with FR-4 dielectric coefficient 4.4. The thickness of substrate for all three antennas having 1.6 mm and thickness of conductor is 0.0175 mm. In these three-design inset feed technique is used for matching the radiating patch with the 50 Ω microstrip feedline. As first, explain the modeling of antenna, which parameters affect the behavior the antenna and how they can be used for the development as design point of view. After then design, a normal antenna and two notch (U-notch and H-notch) antenna have been design and calculate their parameter like as return loss, bandwidth, gain, directivity and the efficiency of antenna. Finally, compare their result in terms of working parameter of 6G and for the application of IoT services.

Inset feed Microstrip Antenna modelling

First a model of the inset feeding is presented. It is shown, which parameters affect the antenna behavior and how they can be used for the development. Figure 3.3 show the assembly of an aperture coupled patch antenna in detail. The patch of length L and width W is placed on a substrate with height h and relative permittivity ε_r.

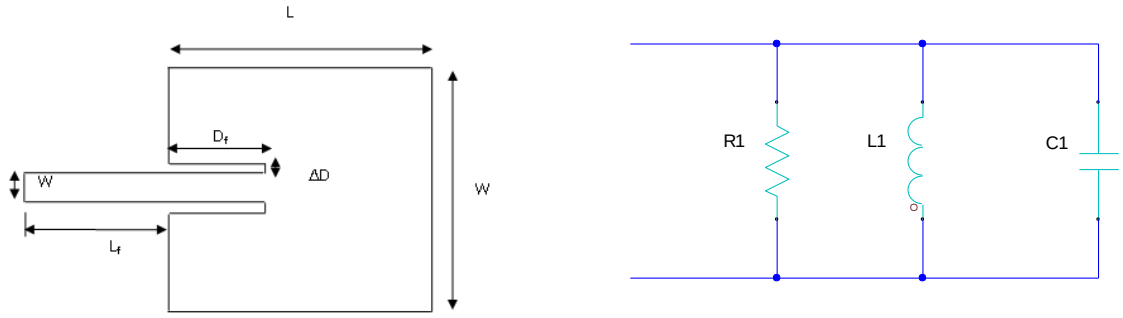

Figure 3.3 Schematic assembly of an aperture coupled patch antenna and its equivalent circuit

Where L_f and W_f is feed length and feed width of antenna. The D_f and ΔD is the deft of feed and cut of feed. The width of the substrates and the ground plane in x and y direction are named G_x and G_y, respectively.
There are different methods for modeling of this antenna [7-9]. In this work transmission line model consider. The equivalent circuit of the transmission line model, derivation and basic concept given by [8].

By Figure. 3.4, Z_{in} is characteristic input impedance of the antenna consisting of the parallel connection of RLC an open-ended line. The microstrip patch is considered as resistance (R1), inductance (L1) and capacitance (C1) as shown. Hence, give results as in equation (3.45).

$$R_1 = \frac{Q_T}{\omega C_1} \quad \text{Eqn. 0.1}$$

$$L_1 = \frac{1}{\omega^2 C_1} \quad \text{Eqn. 0.2}$$

$$C_1 = \frac{\varepsilon_0 \varepsilon_e L W}{2h} \cos^{-2}\left(\frac{\pi y_0}{L}\right) \quad \text{Eqn. 0.3}$$

Where y_0 is feed point location

$$Q_T = \frac{c\sqrt{\varepsilon_e}}{4 f h} \quad \text{Eqn. 0.4}$$

$$Z_P = \frac{1}{\left(\frac{1}{R_1} + \frac{1}{j\omega L_1} + j\omega C_1\right)} \quad \text{Eqn. 0.5}$$

PARAMETER CALCULATION OF MICROSTRIP ANTENNA AT 5.8 GHZ

In this work consider 5.8 GHz frequency, low thickness of feed substrate h=1.6 mm with dielectric constant (ε_r) = 4.4 FR-4 and copper layer thickness t_c = 0.0175 mm.

Feed Line Calculation

Basically, the width of microstrip line consists of dielectric substrate (ε_r), substrate thickness (h_1) and conductor thickness (t_c). For the calculation of feed line width on the characteristic impedance $Z_0(f)$= 50Ω at central frequency of the proposed antenna, simply put the desired parameter in following equation (3.64) and find out desire value i.e W_f = 4.4 mm.

$$W_f = \frac{7.48h}{e\left(z_0 \frac{\sqrt{\varepsilon_r + 1.41}}{87}\right)} - 1.25t_c$$ Eqn. 0.6

Feed Length and Width Calculation

The feed length and width can be calculate based on previous research as equation (3.65-3.66) where λ_0 is the wave length of central frequency of the antenna and find out the desired value D_f= 5.17 mm and ΔD = 0.5 mm.

$D_f \sim (0.1\text{-}0.2)\ \lambda_0$ Eqn. 0.7

$\Delta D \sim 0.10\ L_a$ Eqn. 0.8

Patch Dimension Calculation

Now calculate the length L = 11.75 mm and width W = 15.74 mm by using the equation (3.1-3.4) given by [8].

Ground and Substrate Dimension Calculation

By using following two equations (3.5-3.6) we can find the dimension of ground and substrate of the proposed antenna are G_x = 21.35 mm and G_y =25.34 mm.

Table 3.1 Optimized dimension of the antenna at 5.8 GHz

Parameter	Dimension(mm)
Ground Plane & Substrate Length (G_x)	21.35
Ground Plane& Substrate Width (G_y)	25.34
Patch Length (L)	11.75
Patch Width (W)	15.74
Height of substrate (h)	1.6
Width of feedline (W_f)	4.4
Cut of feed line(ΔD)	0.5
Deft of feed line D_f	5.17

4. Result and Discussion

In this section, three antennas are design. First is at 5.8 GHz and next two antennas designed at 7.125 GHz with help of previous section parameter have considered. The commercially available 3D EM simulator software ANSYS HFSS 2021R1 is used for all simulation work. All simulated result compares and analyzed for bandwidth, gain, directivity and efficiency of antenna point of view. Finally compare discuss the result of in terms of our proposed objective.

INSET FEED PATCH ANTENNA AT 5.8 GHZ

Open ANSYS Electronics Desktop and select HFSS mode with parameter units in mm. Then open the new project and rename them.

Draw Ground Substrate

Draw the box and rename as ground substrate with the dimension of G_x = 21.35 mm and G_y = 25.34 mm. Height of box is h= 1.6 mm with dielectric constant (ε) = 4.4 RF-4 and set position.

Draw Patch Element and feed line

Draw the box and rename as patch with the dimension of L = 11.75 mm and W = 15.74 mm. Height of box is h= 1.6 mm with copper and set position as center. Now draw box with size of W_f = 4.4 mm, L_f = 11 mm. Now draw another box with size of 11x4.9x0.0175 mm and subtract the feed box then join with patch antenna. Now set the color and transparency of element up 70%. Patch antenna with inset feed.

Draw Source Element

Change the position of axis from xy plan to xz plane and draw a rectangular with size 4.4 mm x 1.635 mm as shown in Figure.4.1.

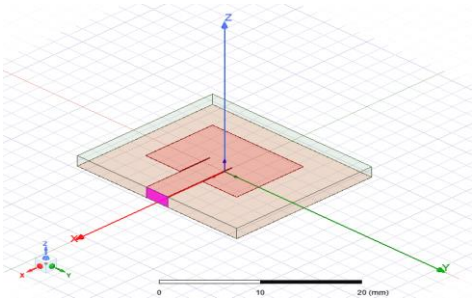

Figure 4.1 3D model of inset microstrip antenna

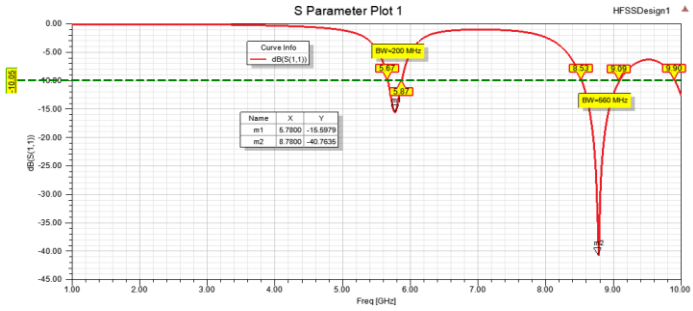

Figure 4.2 Reflection coefficient of microstrip antenna at low frequency band

Assign Boundary Condition and Excitation of Source

Check the position of axis as xy plain. Now assign the boundary condition for all conductor plain as perfect E. Assign the radiating surface as vacuum and solution type considers as terminal. Now assigns excitation with lump port.

Analysis Setup

Assign the analysis at frequency 5.8 GHz, maximum number of passes 20 and maximum delta s = 0.02. Now assign the sweep as fast and distribution for linear step start from 1 GHz to 7 GHz with step size 0.001 GHz.

Simulation

Check validation and click analyze all. After the completion of simulation work plot some parameters like as, S11, VSWR, Smith chart, radiation patterns as well as radiation efficiency.

Return Loss & Smith Chart

The proposed antenna resonates at two frequency 5.78 GHz and 8.78 GHz with a return loss of -15.59 dB and -40.76 dB. Impedance bandwidth obtained 200 MHz and 560 MHz as shown in Figure 4.2. The matching impedance at resonance frequency at 5.78 GHz is real as shown in Figure 4.3 and z parameter shown in Figure 4.4.

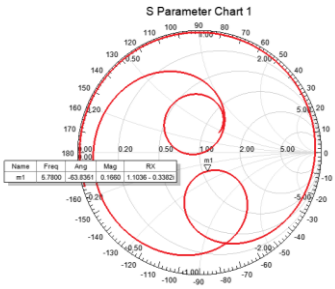

Figure 4.3 Smith chart of microstrip antenna at low frequency band

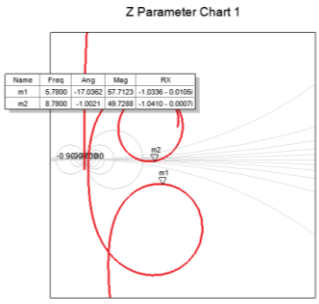

Figure 4.4 Z Parameter of antenna at low frequency band

VSWR

For a microstrip antenna, the VSWR should be between 1 and 2 along the bandwidth of efficiency. The antenna voltage standing wave ratio (VSWR) can be observing 1.39 and 1 at 5.78 and 8.78 GHz respectively shown in Figure.4.5.

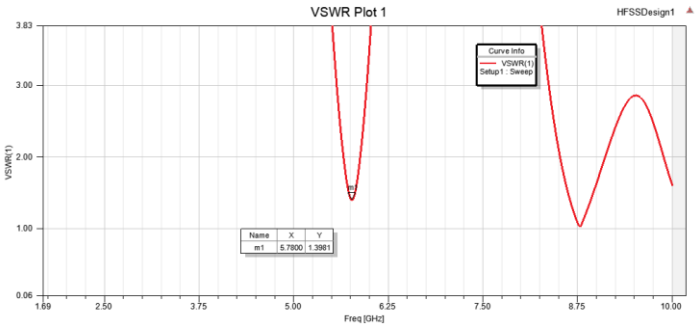

Figure 4.5 VSWR of microstrip antenna at low frequency band

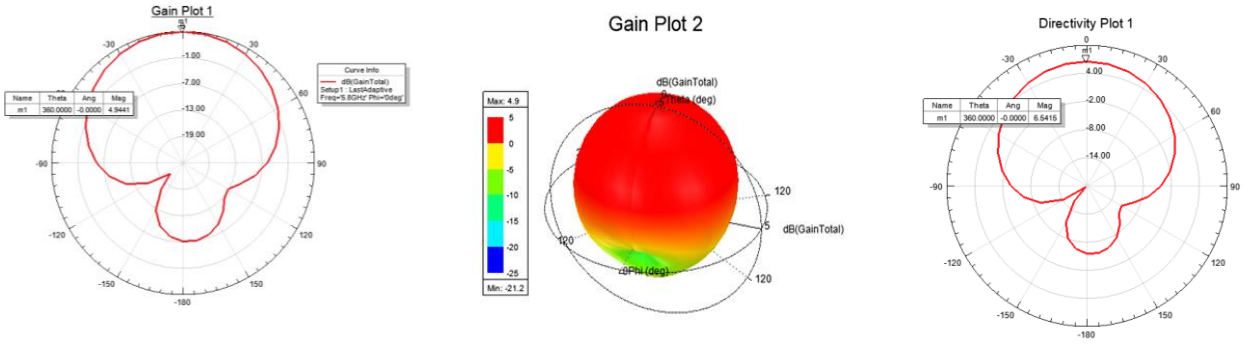

Figure 4.6 2D -3D Gain plot and directivity of microstrip antenna at low frequency band

Gain & Directivity

Antenna has the maximum gain 4.9 dB, Directivity of antenna is 6.54 dB shown in Figure.4.6.

Table 4.1 Summary of simulated result at low frequency band

Antenna Parameter	Values
S_{11}	-20.4438
VSWR	1.21
Bandwidth	200 MHz
Gain	4.9 dB
Directivity	6.54 dB
Efficiency	69.22%

DESIGN OF MID FREQUENCY ANTENNA AT 7.125 GHZ

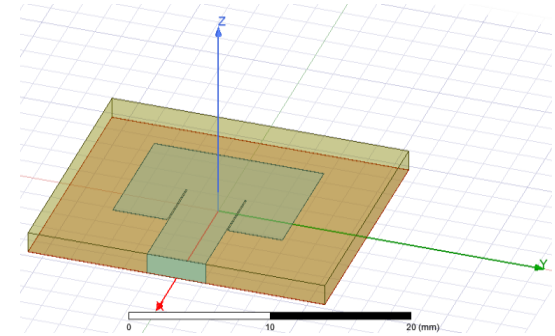

Figure 4.7 Inset microstrip antenna at mid frequency band

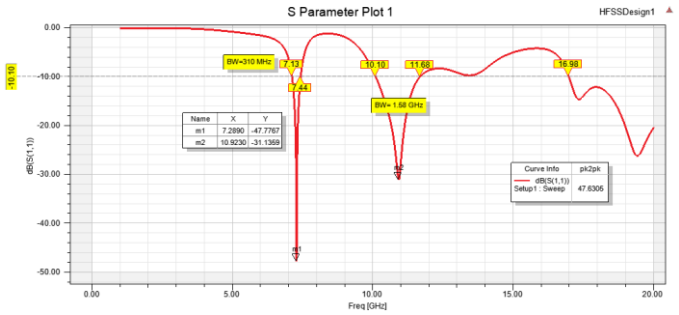

Figure 4.8 Reflection coefficient of microstrip antenna at mid frequency band

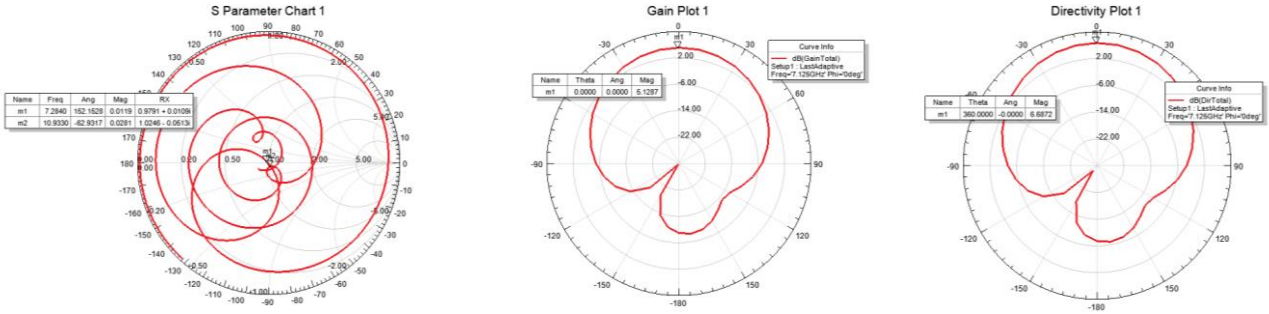

Figure 4.9 Smith chart Gain and Directivity plot of microstrip antenna at mid frequency band

DESIGN INVERTED U-NOTCH MICROSTRIP ANTENNA

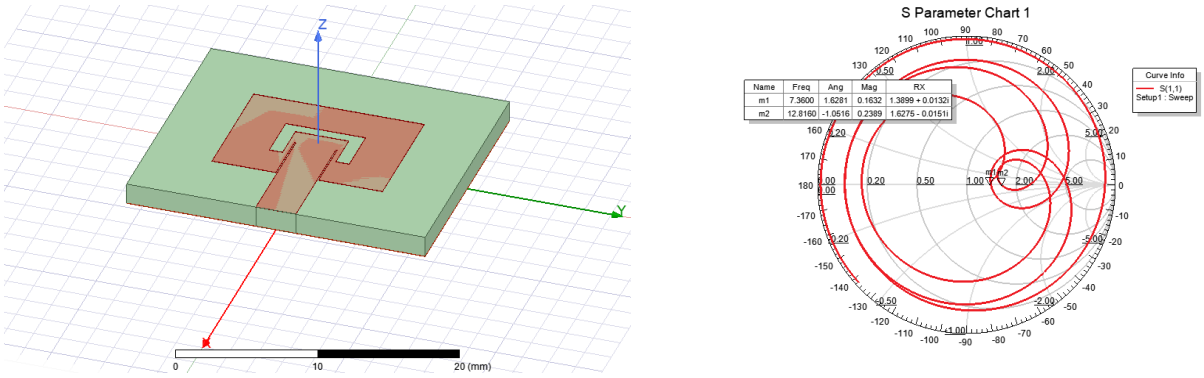

Figure 4.10 3D model and smith chart of inverted U-notch microstrip antenna

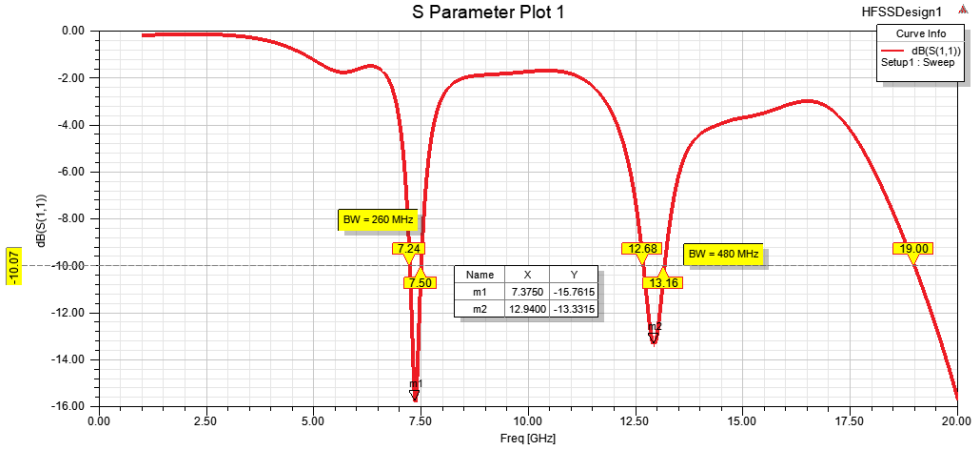

Figure 4.11 Reflection coefficient of inverted U-notch microstrip antenna

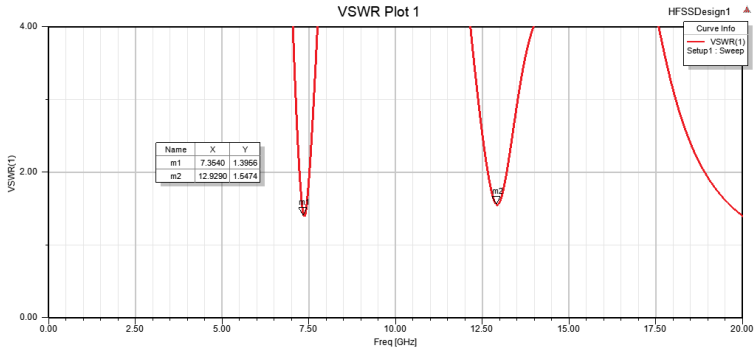

Figure 4.12 VSWR of inverted U-notch microstrip antenna

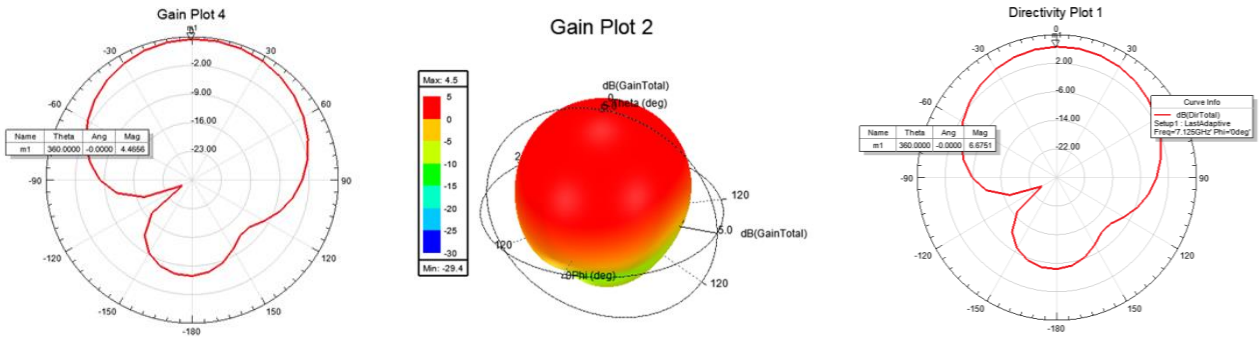

Figure 4.13 2D and 3D Gain plot and Directivity of inverted U-notch microstrip antenna

RESULT ANALYSIS

Here we can see that the antenna design at 5.8 GHz gives two resonance frequency 5.78 GHz and 8.78 GHz having -15.59 dB and -4076 dB return loss respectively. Whereas antenna design on mid frequency band at 7.125 GHz also gives two resonance frequency 7.289 GHz and 10.92 GHz having return loss -47.0 dB and -31.159 dB respectively. Similarly, inverted U-notch antenna design on same mid frequency band and gives two resonance 7.38 GHz and 12.94 GHz having -15.61 dB and -13.34 dB respectively. The voltage standing ratio are all three antennas are less than 2. The impedance bandwidth of antenna first are 200 MHz and 560 MHz, second antenna gives the impedance bandwidth 310 MHz and 1.58 GHz, third antenna that is inverted U-notch gives 260 MHz and 480 MHz impedance bandwidth respectively. The gain of first, second and third antenna are 4.94 dB, 5.12 dB and 4.5 dB and directivity 6.54 dB, 6.687 dB, 6.675 dB respectively. The all three-antenna radiation efficiency 69.22 %, 69.85 % and 60.12 % respectively. The result of all three antenna compare with the requirement of 6G antenna and IoT services. Therefor these antennas appropriate for 6G and IoT services. The summary of all three antenna which have design are shown in Table 4.2.

Table 4.2 Summary of the simulated result of the antenna

Parameter Antenna	Resonance frequency	S_{11}	VSWR	Bandwidth	Gain	Directivity	Efficiency	Application
At 5.8 GHz	5.78 GHz 8.78 GHz	-15.59 dB -40.76 dB	1.39 1	200 MHz 560 MHz	4.94 dB	6.54 dB	69.22 %	IoT
At 7.125	7.29 GHz 8.78 GHz	-47.0 dB -31.16 dB	1.09 1.63	310 MHz 1.5 GHz	5.12 dB	6.68 dB	69.85 %	Advance IoT
At 7.125 (Inverted U-Notch)	7.38 GHz 12.94 GHz	-15.61 dB -13.34 dB	1.39 1.54	260 MHz 480 MHz	4.5 dB	6.675 dB	60.12 %	Advance IoT

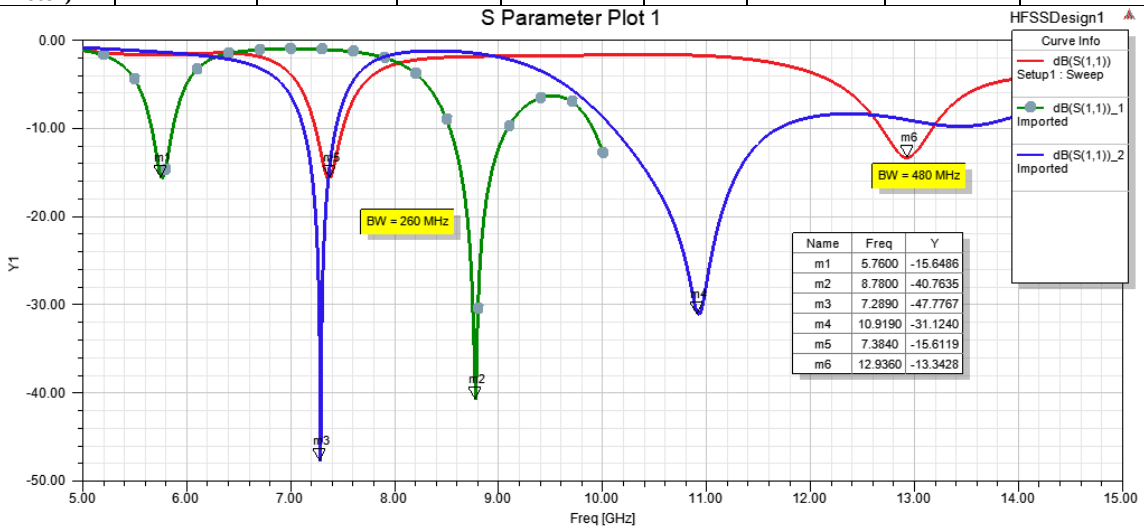

Figure 4.14 Summary of reflection coefficient of antenna all antenna

Figure 4.27 shows the compiled result of reflection coefficient on all three antenna. The line of bubble with green color represent antenna first design at 5.8 GHz. The line of blue color represent antenna second design at 7.125 GHz. The line of red color represents inverted U-notch antenna design at 7.125 GHz that is antenna third.

Also compare our design antenna with previous work as shown in Table 4.3.

Table 4.3 Compare with previous work

Reference	Resonance frequency	S_{11}	ε_r	Bandwidth	Gain	Directivity	Efficiency	Application
[1]	868 MHz	-34.3 dB	FR-4	20 MHz	-	-	-	IoT
[3]	5.755 GHz	-20.32 dB -26.56 dB	FR-4	134.1 MHz 167.6 MHz	1.83 dB 2.54 dB	-	-	IoT
antenna (1)	5.78 GHz 8.78 GHz	-15.59 dB -40.76 dB	FR-4	200 MHz 560 MHz	4.94 dB	6.54 dB	69.22 %	IoT
antenna (2)	7.29 GHz 8.78 GHz	-47.0 dB -31.16 dB	FR-4	310 MHz 1.5 GHz	5.12 dB	6.68 dB	69.85 %	Advance IoT
antenna (3)	7.38 GHz 12.94 GHz	-15.61 dB -13.34 dB	FR-4	260 MHz 480 MHz	4.5 dB	6.675 dB	60.12 %	Advance IoT

From Table 4.3 as per compared with previous work our all three antenna gives the better result as bandwidth more than 200 MHz on the same substrate material used. Antenna 1 gives two resonance frequency 5.78 GHz and 8.78 GHz having of bandwidth of 200 MHz and 560 MHz respectively. Antenna 2 also gives two resonance frequency 7.29 GHz and 8.78 GHz having of bandwidth of 310 MHz and 1500 MHz respectively. Antenna 3 also gives two resonance frequency 7.38 GHz and 12.94 GHz having of bandwidth of 260 MHz and 480 MHz respectively.

Here all three antenna gives better gain and directivity 2.54 dB. Antenna1 gives the gain 4.94 dB and directivity 6.54 dB. Antenna2 gives the gain 5.12 dB and directivity 6.68 dB. Antenna3 gives the gain 4.5 dB and directivity 6.675 dB. All three-antenna having more than 60% of resistance efficiency.

Over all our antennas are full fill the basic requirement for ^G and IoT application also. Here antenna 1 will work for IoT application whereas antenna2 antenna 3 will work for advance IoT application for 6G band.

5. Conclusion

In this section, concluded the modelling, design and simulated result point of view. Three antenna design first for 6G low frequency band at 5.8 GHz and two for 6G mid frequency band at 7.125 GHz. All the antenna having same substrate material as FR-4 epoxy having dielectric coefficient 4.4 and substrate thickness 1.6 mm. The commercially available ANSYS HFSS 2021R1 full wave EM software used for simulation work. The antenna gets the simulation result in the term of reflection coefficient, VSWR, gain and directivity point of view. Further, compare the result in terms of reflection coefficient, VSWR, gain and directivity. Here all three-antenna having bandwidth more than 160 MHz that is all antenna work for 6G application and good appropriate for IoT services. All the antenna gets gain more than 4 dB and also directivity of all three antenna gives more than 6 dB, therefor all three-antenna design in this work as a good option for 6G and IoT applications.

REFERENCES :

1. Anchidin, L.; Lavric, A.; Mutescu, P.-M.; Petrariu, A.I.; Popa, V., “The Design and Development of a Microstrip Antenna for Internet of Things Applications”, Sensors 2023, 23,1062. https://doi.org/10.3390/ s23031062
2. Narayan Krishan Vyas and Dr. Mohammad Salim, “High gain Antenna Design for 6G wireless Applications,” research square, 2022.
3. doi: https://doi.org/10.21203/rs.3.rs-2292556/v1
4. Adewale Ayomikun Elijah and Mastaneh Mokayef, “Miniature microstrip antenna for IoT application,” Materials Today: Proceedings, ELSEVIER, pp. 2-5, 2020 (Cross reference).
5. Chen, X., Abdullah, M., Li, Q., Li, J., Zhang, A., & Svensson, T. “Characterizations of mutual coupling effects on switch-based phased array antennas for 5G millimeter-wave mobile communications,” IEEE Access, 7, 31376-31384, 2019.
6. Qamar, F., Hindia, M. H. D., Dimyati, K., Noordin, K. A., Majed, M. B., Abd Rahman, T., & Amiri, I. S. “Investigation of future 5G-IoT millimeter-wave network performance at 38 GHz for urban microcell outdoor environment,” Electronics, 8(5), 495, 2019.
7. Hui, D., Sandberg, S., Blankenship, Y., Andersson, M., & Grosjean, L. “Channel coding in 5G new radio: A tutorial overview and performance comparison with 4G LTE,” IEEE vehicular technology magazine, 13(4), 60-69, 2018.
8. Prutha P. Kulkarni, Antennas for IoT, Artech House, 2023.
9. D.G. Fang, Antenna theory and microstrip antennas, CRC Press, 2009.
10. A.B. Constantine, Antenna theory: analysis and design. Microstrip Antenna, 3rd edition, John Wiley & Sons, 2005.
11. Garg, R.; Bhartia, P.; Bahl, I.J.; Ittipiboon, A. Microstrip Antenna Design Handbook; Artech House: Norwood, MA, USA, 2001.
12. Ansys HFSS|3D High Frequency Simulation Software. Available online: https://www.ansys.com/products/electronics/ansys-hfss (accessed on 22 December 2022).
13. Harsh Tataria, Andreas F. Molisch, Mischa Dohler, Henrik Sjöland, and Fredrik Tufvesson,’ 6G Wireless Systems: Vision, Requirements, Challenges, Insights, and Opportunities’, Proceedings of the IEEE | Vol. 109, No. 7, July 2021.
14. B. Aqlan, M. Himdi, L. L. Coq, and H. Vettikalladi, "Sub-THz Circularly Polarized Horn Antenna Using Wire Electrical Discharge Machining for 6G Wireless Communications," IEEE Access, vol. 8, pp. 117245-117252, 2020.
15. Saad W, Bennis M, Chen M, A vision of 6G wireless systems: applications, trends, technologies, and open research problems IEEE Netw2020, 34(3), 134-142.
16. K. B. Letaief, W. Chen, Y. Shi, J. Zhang, and Y. J. A. Zhang,“The Roadmap to 6G: AI Empowered Wireless Networks,” IEEE Commun. Mag., vol. 57, no. 8, pp. 84–90, Aug. 2019, doi:10.1109/MCOM.2019.1900271.
17. X. Jia et al., "Antenna with Embedded Die in Glass Interposer for 6G Wireless Applications," in IEEE Transactions on Components, Packaging and Manufacturing Technology, vol. 13, no. 2, pp. 219-229, Feb. 2023, doi: 10.1109/TCPMT.2023.3251725.
18. J. V, K. N and A. S, "Channel Estimation Method in Reconfigurable Intelligent Surfaces for 6G Wireless Systems," 2023 International Conference on Sustainable Communication Networks and Application (ICSCNA), Theni, India, 2023, pp. 73-80, doi: 10.1109/ICSCNA58489.2023.10370048.
19. R. K. Mahapatra et al., "Compact wideband microstrip circular patch antenna for 6G application," 2023 International Conference on Advancement in Computation & Computer Technologies (InCACCT), Gharuan, India, 2023, pp. 832-837, doi: 10.1109/InCACCT57535.2023.10141831.
20. Omi, M. S. I. Sagar, M. M. H. Sajeeb, B. Younes, T. Karacolak and P. Sekhar, "A New Analytically Designed UWB Microstrip Patch Antenna for Future 5G and 6G Applications," 2023 United States National Committee of URSI National Radio Science Meeting (USNC-URSI NRSM), Boulder, CO, USA, 2023, pp. 62-63, doi: 10.23919/USNC-URSINRSM57470.2023.10043157.
21. S. Bhutiani and K. Tadas, "An Improved Design of 6G Microstrip Patch Antenna with a High Reflection Coefficient and Working Frequency of 5.8 GHz," 2023 IEEE International Conference on ICT in Business Industry & Government (ICTBIG), Indore, India, 2023, pp. 1-3, doi: 10.1109/ICTBIG59752.2023.10456065.
22. M. A. Saeed and A. Nwajana, "U-Shaped Terahertz Microstrip Patch Antenna for 6G Future Communications," 2023 7th International Electromagnetic Compatibility Conference (EMC Turkiye), İstanbul, Turkiye, 2023, pp. 1-4, doi: 10.1109/EMCTurkiye59424.2023.10287461.

23. N. Mayer, S. Ashraf, J. A. Sheikh and A. A. Balkhi, "Implementation of SRR Loaded Frequency Reconfigurable Antenna for 5G and IoT Wireless Applications," 2023 10th IEEE Uttar Pradesh Section International Conference on Electrical, Electronics and Computer Engineering (UPCON), Gautam Buddha Nagar, India, 2023, pp. 741-746, doi: 10.1109/UPCON59197.2023.10434466.
24. D. Prasetyo, H. Vidyaningtyas, D. Hamdani and A. Munir, "Bandwidth Enhancement of a Planar Monopole Antenna Using CMA-ES Optimizer for B5G/6G Applications," 2023 28th Asia Pacific Conference on Communications (APCC), Sydney, Australia, 2023, pp. 407-411, doi: 10.1109/APCC60132.2023.10460664.
25. S. Tiwari, M. Kumari, V. Kikan, R. Gill, A. Kumar and M. Sharma, "A Novel Design Evolution of mmWave W-D Bands Modified Rectangular Patch Antenna with Circular and Rectangular Slots for Future IoT Applications," 2023 6th International Conference on Contemporary Computing and Informatics (IC3I), Gautam Buddha Nagar, India, 2023, pp. 1843-1848, doi: 10.1109/IC3I59117.2023.10397852.
26. P. Kumar, A. Raj and D. Mandal, "Design and Fabrication of Sierpinski Fractal-Based MIMO Antenna for Sub 6GHz and IOT Applications," 2023 2nd International Conference on Futuristic Technologies (INCOFT), Belagavi, Karnataka, India, 2023, pp. 1-5, doi: 10.1109/INCOFT60753.2023.10425370.